Am J Transl Res 2017;9(4):1943-1955
www.ajtr.org /ISSN:1943-8141/AJTR0041122

Original Article

Histone H3K14 hypoacetylation and H3K27 hypermethylation along with HDAC1 up-regulation and KDM6B down-regulation are associated with active pulmonary tuberculosis disease

Yung-Che Chen[1,3], Tung-Ying Chao[1], Sum-Yee Leung[1], Chung-Jen Chen[2], Chao-Chien Wu[1], Wen-Feng Fang[1], Yi-Hsi Wang[1], Huang-Chih Chang[1], Ting-Ya Wang[1], Yong-Yong Lin[1], Yi-Xin Zheng[1], Meng-Chih Lin[1], Chang-Chun Hsiao[3]

[1]Division of Pulmonary and Critical Care Medicine, [2]Division of Rheumatology, Kaohsiung Chang Gung Memorial Hospital and Chang Gung University College of Medicine, Kaohsiung, Taiwan; [3]Graduate Institute of Clinical Medical Sciences, College of Medicine, Chang Gung University, Center for Shockwave Medicine and Tissue Engineering, Kaohsiung Chang Gung Memorial Hospital, Taiwan

Received October 3, 2016; Accepted November 26, 2016; Epub April 15, 2017; Published April 30, 2017

Abstract: The aim of this study is to determine the roles of global histone acetylation (Ac)/methylation (me), their modifying enzymes, and gene-specific histone enrichment in active pulmonary tuberculosis (TB) disease. Global histone H3K27me3, H3K27me2, H3K9me3, H3K9Ac, and H3K14Ac expressions, and their modifying enzyme expressions, including KDM1A, KDM6B, EZH2, HDAC1, and HDAC2, were assessed in blood leukocytes from 81 patients with active pulmonary TB disease and 44 matched healthy subjects (HS). *TLR2*, *TNF-α*, *IFN-γ*, and *IL12B*-specific histone enrichment of peripheral blood mononuclear cells was measured by chromatin immunoprecipitation method. We found that Global H3K14Ac was decreased and H3K27me2 was increased in TB patients as compared with that in HS. TB patients with low H3K14Ac had lower one-year survival. Global H3K27me3 was increased in TB patients with high bacterial burden, or systemic symptoms as compared with that in those without the attribute or HS. HDAC1 gene/protein expressions were increased in TB patients as compared with that in HS, whereas KDM6B gene/protein expressions were decreased. Global H3K27me2, HDAC1 and KDM6B protein expressions were all reversed to normal after 6-month anti-TB treatment. *TNF-α/IL12B* promoter-specific H3K14Ac and *TNF-α/IL12B/IFN-γ* promoter-specific H3K27me2 enrichment were all decreased in 10 TB patients as compared with that in 10 HS. Among them, *IL12B*-specific H3K27me2 enrichment was reversed to normal after treatment, while the other 4 remained depressed. In conclusions, H3K14 hypoacetylation and H3K27 hypermethylation play a role in the development of active pulmonary TB disease or its clinical phenotypes, probably through up-regulation of HDAC1 and down-regulation of KDM6B, respectively.

Keywords: Pulmonary tuberculosis, histone H3K14 acetylation, histone H3K27 methylation, HDAC1, KDM6B, interleukin 12B

Introduction

It is estimated that 9.0 million people developed tuberculosis (TB) and 1.5 million died from this disease in 2013 despite ongoing research efforts and ever-increasing knowledge [1]. *Mycobacterium tuberculosis* (Mtb) is able to manipulate both the innate and acquired immune response of the host, including macrophage, natural killing cell, and antigen-specific $CD4^+$/$CD8^+$ T cell, through several pathogen recognition receptors, such as toll-like receptor (TLR) 2/4/8/9, which trigger early tumor necrosis factor-α (TNF-α)/interferon-γ (IFN-γ) and late interleukin 12 B (IL12-B) cytokine release. It is still poorly understood about the earliest encounters between Mtb and the human immune systems, so that we are far from developing the diagnostic and therapeutic approaches that would reduce the severity of this global epidemic [2, 3].

The development and differentiation of immune cells for defense against infection diseases are

attributed in part by dynamic epigenetic modulations, including DNA methylation and histone modification [4]. In our previous study, we found that DNA hypermethylation of certain CpG sites over *TLR2* promoter region is associated with active pulmonary TB or its clinical phenotypes, probably through the down-regulation of TLR2 expression [5, 6]. The methylation (me) of the lysine (K) residues of histone H3, such as H3K9 and H3K27, is thought to be a code for transcriptional repression, whereas the methylation of histone H3K4, H3K36 and H3K79, and the acetylation (Ac) of histone H3, especially of H3K9, H3K14 and H3K27, function as an active transcriptional code [7, 8]. A variety of histone lysine methyltransferases (KMT) and histone lysine demethylases (KDM) are involved in controlling the state of histone methylation, while the state of histone acetylation are governed by histone acetyltransferase (HAT) and histone deacetylase (HDAC) [9]. Class I HDAC, including 1, 2, 3, and 8, catalyze histone deacetylation over a wide spectrum of H3 [4]. The Jumonji domain containing-3 (JMJD3, KDM6B) has been identified as H3K27 demethylases that catalyze the demethylation of H3K27me2/3, while enhancer of zeste 2 polycomb repressive complex 2 subunit (EZH2) catalyzes methylation of H3K27 and mediates gene silencing of target genes [10, 11]. Lysine-specific demethylase 1 (LSD1; KDM1A) has been reported to repress and activate transcription by mediating histone H3K4-me and H3K9me demethylation, respectively [12].

Based on previous findings of the relationships between histone modifications and infectious diseases, such as herpes virus and aspergillus infections [13-23], it is hypothesized that patients with active pulmonary TB have aberrant global histone methylation/acetylation patterns, which may affect the development and clinical phenotypes of TB. To test this hypothesis, this prospective cohort study checked the global H3K27 trimethylation (me3), H3K27 dimethylation (me2), H3K9me3, H3K9Ac, and H3K14Ac, and their corresponding enzymes, including KDM6B, KDM1A, EZH2, HDAC1, and HDAC2, of blood leukocyte in 81 patients with active pulmonary TB and 44 healthy subjects (HS). Furthermore, we checked several immune gene-specific H3K14Ac and H3K27me2 enrichment of peripheral blood mononuclear cells (PBMCs) in 10 TB patients before and after 6-month anti-TB treatment, and 10 HS.

Patients and methods

Study subjects

The study population consisted of 81 patients with newly diagnosed pulmonary TB who were undergoing anti-TB treatment at the Pulmonary Department of the Chang Gung Memorial Hospital (Kaohsiung, Taiwan) from March 2011 to December 2013. The criteria for enrollment were clinical and radiological findings indicating pulmonary TB, and at least 1 positive Mtb culture from sputum examinations or one bronchial washing specimen obtained by bronchoscopy. Patients with HIV or concomitant infection other than Mtb were excluded. Acid fast bacilli (AFB) smears and mycobacterial cultures were performed, and standard posterior-anterior chest X-rays (CXR) were assessed for disease severity as previously described.

Forty-four unrelated healthy subjects (HS) were recruited from the Center of Health Examination of Kaohsiung Chang Gung Memorial Hospital. The criteria for enrollment were the absence of pulmonary lesions on CXR examination and a negative history of TB disease. The Chang Gung memorial hospital's institutional review board approved the study protocol (99-3784B/101-4408C), and all subjects provided informed written consents before blood sampling. All patients were treated in according to the American Thoracic and Infectious Society guidelines for the management of TB, and received directly observed treatment, short course strategy.

Isolation of leukocyte RNA and protein from whole blood samples

Leukocytes were isolated from heparinized blood of all study subjects using a two-layer Ficoll-Histopaque density gradient centrifugation (Histopaque 1.077 and 1.119; Sigma Diagnostics, St.Louis, MO) method. Blood samples at diagnosis before anti-TB treatment were obtained and analyzed from all TB patients and HS, and after six months of anti-TB treatment (month 6) from 28 patients. Samples were stored in RNA*later*® RNA Stabilization Solution (Ambion®) at -80°C until analysis. An RNeasy® Plus Mini Kit (Qiagen, Hilden, Germany) was

Table 1. Primer sequences for assay quantitative real-time polymerase chain reactions used in the present study

Gene name	Primer sequences	
KDM1A (LSD1)	Forward	5'-CATCATGGTGCAAGAAGAGC
	Reverse	5'-ATGTGGGAAAGGCAGACAAG
KDM6B (JMJD3)	Forward	5'-CACCCACTGTGGTCTGTTGT
	Reverse	5'-TGTCTCCGCCTCAGTAACAG
HDAC1	Forward	5'-CGGTGCTGGACATATGAGAC
	Reverse	5'-TGGTCCAAAGTATTCAAAGTAGTCA
HDAC2	Forward	5'-CCAGATGTTCTGGCATCCTC
	Reverse	5'-ACAGCCCCTGTTGTCCTGT
EZH2	Forward	5'-CGCTTTTCTGTAGGCGATGT
	Reverse	5'-ACAGCCCCTGTTGTCCTGT
TLR2 promoter	Forward	5'-TCCAGAGTTCCCTCCGGC
	Reverse	5'-GCCCGGGACTAGGAAGTAAGC
TNF-α promoter	Forward	5'-GGGAGTGTGAGGGGTATCCT
	Reverse	5'-AACCAGCGGAAAACTTCCTT
IFN-γ promoter	Forward	5'-TGTGTGCCAAGCTAAGCAGT
	Reverse	5'-AGAGTTGCATTTGGTTCCATT
IL12B promoter	Forward	5'-TGAGAGCTTCCACCCCTAAA
	Reverse	5'-CAAGTCTACCAGGGGTGCAT
GAPDH	Forward	5'-GAAGAGCCAAGGACAGGTAC
	Reverse	5'-CAACTTCATCCACGTTCACC

used for isolation of high quality total RNA, and treated with DNase according to the manufacture protocol.

Determination of KDM1A, KDM6B, EZH2, HDAC1, and HDAC2 gene expressions of isolated blood leukocytes using quantitative reverse-transcriptase polymerase chain reaction (RT-PCR)

To determine the expressions of *KDM1A, KDM6B, EZH2, HDAC1*, and *HDAC2* of the isolated leukocytes, the gene expressions were analyzed using quantitative RT-PCR in a 32-well format. The house keeping gene *GAPDH* was chosen as an endogenous control to normalize the expression data for each gene. All PCR primers (random hexamers) were designed and purchased from Roche according to the company's protocols (www.roche-applied-science.com), and their sequences are given in **Table 1**. RNA samples were treated with DNAfree to remove contaminating genomic DNA. A total of 300 ng RNA was used for synthesis of first strand cDNA with QuantiTectReverse Transcription Kit (QIAGEN, Germany). A total of 5 μl of the reverse transcription reaction was added to 5 μl of master mix (QIAGEN, SYBR Green PCR kit; Roche, Germany). The PCR reactions with 45 cycles of amplification were run in a Roche LightCycle 480 machine. Single real time PCR experiment was carried out on each sample for each target gene, because the Roch Light CyclerQuantiFast R system has shown high reproducibility. Relative expression levels were calculated using the ΔΔCq method with the median value for the control group as the calibrator.

Measurement of global H3K27me3, H3K27me2, H3K9me3, H3K9Ac, H3K14Ac, KDM1A, KDM6B, EZH2, HDAC1, and HDAC2 protein expressions in the blood leukocytes using ELISA

Protein levels of global H3K27me3, H3K27me2, H3K9me3, H3K9Ac, H3K14Ac, KDM1A, KDM6B, EZH2, HDAC1, and HDAC2 in the blood leukocytes were assessed by a commercial ELISA method (Epigentek, USA, and R&D systems, Minneapolis, MN). Briefly, 40 μl dye (Bio-Rad Protein Assay Dye Reagent Concentrate #500-0006) was added to 10 μl bovine serum albumin with serial dilution to generate a standard curve for total protein concentration by measuring values at OD 595 nm. Accordingly, protein lysate equivalent to 20 ng of total protein was used for each protocol in ELISA analysis.

Determining gene-specific H3K14Ac and H3K27me2 by Chromatin immunoprecipitation (ChIP) assay-quantitative RT-PCR

3-5 $\times 10^5$ PBMCs from 10 TB patients at diagnosis, 10 TB patients after 6-month anti-TB treatment, and 10 HS were harvested and fixed with 1% formaldehyde at room temperature, followed by glycine to stop the crossing linking reaction. Cells were re-suspended in cell lysis buffer containing 1X Protease Inhibitor Cocktail II (200X, Millipore, USA). Extracts were sonicated using a Standard Sonicator (Diagenode Bioruptor) set on "HIGH" for 120 cycles of 20 sec ON and 10 sec OFF to achieve chromosome

Table 2. Demographic and clinical characteristics in the 81 culture positive pulmonary tuberculosis (TB) patients, and 44 matched healthy subjects

	All pulmonary TB patients N = 81	All healthy subjects N = 44	*p* value*	Follow-up TB patients after 6 month treatment N = 28
Age, years	59.8±17.4	57.2±10.9	0.163	54.1±18.2
Male sex, n (%)	61 (75.3)	29 (70.7)	0.587	20 (71.4)
Co-morbidity, n (%)				
Hypertension	15 (18.5)	11 (26.8)	0.29	8 (28.6)
Diabetes mellitus	27 (33.3)	10 (24.4)	0.31	12 (42.9)
COPD/Asthma	11 (13.6)	2 (4.9)	0.141	4 (14.3)
Chronic hepatitis	17 (21)	6 (14.6)	0.397	4 (14.3)
Chronic kidney disease	8 (9.9)	2 (4.9)	0.342	1 (5.3)
Heart failure	4 (4.9)	2 (4.9)	0.988	1 (3.6)
Alcoholism, n (%)	4 (5)	3 (6.8)	0.92	2 (7.1)
Smoking history, n (%)	21 (25.9)	13 (31.7)	0.501	7 (25)
Sputum smear at diagnosis, n (%)				
Acid fast bacilli 0	28 (33.8)			12 (44.4)
Acid fast bacilli 1+	24 (30)			11 (40.7)
Acid fast bacilli 2+	9 (11.3)			1 (3.7)
Acid fast bacilli 3+	8 (10)			2 (7.4)
Acid fast bacilli 4+	12 (15)			1 (4)
Drug-resistant TB, n (%)	12 (12.1)			3 (17.6)
CXR at diagnosis, n (%)				
Far advanced lesions	40 (40.4)			8 (36.4)
Minimal to moderate	59 (59.6)			13 (60)
Systemic symptoms, n (%)	21 (25.9)			10 (40)
Fever	9 (11.1)			7 (28)
Body weight loss	12 (14.8)			4 (16)

*Comparisons between all TB patients and all healthy subjects by independent t-test or chi-square test as indicated.

fragment lengths of 200-400 bp. 100 μl sonicated cell extract were diluted in 400 μl ChIP Dilution Buffer (EZ-Magna ChIP™ A/G kit, Millipore, USA), and incubated with 1 μg of anti-H3K14Ac or anti-H3K27me2 (Millipore, USA) at 4°C for 1 hour while rotating. Two aliquots were reserved as "controls"-one incubated without antibody and the other with non-immune Mouse IgG (25 ug, Millipore, USA). Protein A/G magnetic beads were added and incubated at 4°C overnight while rotating. Cross-linking of the immunoprecipitated chromatin complexes and "input controls" (10% of the total soluble chromatin) were reversed by heating the samples at 62°C for 4 hours, followed by Proteinase K 1 μL incubation (Millipore, USA). The DNA were purified by spin column and stored at -20°C.

For real-time RT-PCR analysis, amplification of *TLR2, TNF-α, IFN-γ,* and *IL12B* promoter DNA was performed using the TaqMan reagent kit (PerkinElmer Life Sciences). The PCR primers for the four selected gene promoters located from -300 to +30 bp of their transcription start site (TSS) were listed in **Table 1**. The conditions for the reaction were: 50°C, 2 min; 94°C, 10 min, then 95°C, 20 s; 60°C, 30 s for 50 cycles. Resulting PCR products were measured and elaborated by the sequence detector ABI GeneAmp PCR System 9700 (PerkinElmer Biosystems). Primers were designed by Primer Express software (PerkinElmer). For the detection of the four gene promoter DNA after immunoprecipitation (IP) of H3K14Ac or H3K27me2, changes between PBMCs from TB and HS among different IP conditions were based on the shift of threshold cycle (C_T), the fractional cycle number at which the amplified target reaches a significant threshold. The higher the starting copy number of the target, the sooner a significant increase in signal will be

observed as lower C_T number. Histone enrichment was compared by percent input method, in which signals obtained from the ChIP were divided by signals obtained from an input sample, and were calculated by the equation of 100*2^ (adjusted C_T (input) - C_T (IP)) [24, 25].

Statistical analysis

Continuous values were expressed as mean ± standard deviation (SD). The differences between two groups were analyzed by independent Student's t, paired t, Mann-Whitney U, and chi-square tests, where appropriate. Multiple linear regression analysis was used to minimize the effects of confounding factors on the subgroup comparisons of continuous variables, and to provide adjusted *p* values and 95% confidence intervals (CI). Correlations between two continuous variables were evaluated using Spearman's correlation coefficient. Multivariate Cox proportional hazards regression analysis with stepwise forward selection was used to evaluate independent prognostic factors associated with survival, with age, smoking history, and co-morbidities as covariates. Differences in survival among groups were analyzed with the Log-Rank test. To assess diagnostic accuracy, the candidate biomarker was analyzed by area under the receiver operating characteristic curves (AUC). The null hypothesis was rejected at $P < 0.05$. Analyses were performed using the SPSS 15.0 statistical software (SPSS Corp., Chicago, IL).

Results

Demographics of the participants

A total of 125 subjects, including 81 patients with sputum culture positive pulmonary TB patients and 44 healthy subjects, were enrolled and analyzed. Characteristics of cases and controls are listed in **Table 2**. The study population was all Asian in ethnicity. Age, male sex ratio, smoking history, alcoholism history, and co-morbidity were all matched between the 2 groups.

Differential global histone methylation/acetylation patterns related to active pulmonary TB disease and its clinical phenotypes

Global H3K14Ac was significantly decreased (4.4±2.6 versus 6.26±1.16 ng/μl, P < 0.001, **Figure 1A**) and global H3K27me2 (3.68±9.8 versus 1.12±1.37 ng/μl, P = 0.004, **Figure 1B**) was increased in the TB patients at diagnosis as compared with that in the healthy subjects, while global H3K27me3 (0.039±0.029 versus 0.033±0.023 ng/μl, P = 0.285), H3K9me3 (0.64±0.98 versus 0.89±0.29 ng/μl, P = 0.232), and H3K9Ac (0.73±1.97 versus 0.61±0.26 ng/μl, P = 0.713) were not significantly different between the TB and HS groups. TB patients with low H3K14Ac expression (< 4 ng/μl) had lower one-year survival (all cause mortality rate 19.2% versus 0%, P = 0.008 by Log-Rank test, **Figure 1C**) than those with high H3K14Ac expression (≥ 4 ng/μl). Subgroup analyses revealed that global H3K27me3 was significantly increased in the TB patients with high bacterial burden (sputum AFB = 2+, 3+, or 4+; n = 29; 0.046±0.029 ng/μl) as compared with either that in those with low bacterial burden (sputum AFB = 0 or 1+, n = 52; 0.034±0.027 ng/μl, adjusted P = 0.039) or that in the HS (adjusted P = 0.015, **Figure 1D**). Moreover, global H3K27me3 was significantly increased in the TB patients with systemic symptoms at diagnosis (fever or body weight loss; n = 33; 0.046±0.027 ng/μl) as compared with either that in those without systemic symptoms (n = 48; 0.032±0.028 ng/μl; adjusted P = 0.029) or that in the HS (adjusted P = 0.018, **Figure 1E**). Global H3K14Ac was negatively correlated with H3K27me3 (r = -0.433, P < 0.001, **Figure 1F**). Both global H3K27me3/H3K14Ac ratio (0.13±0.5 versus 0.007±0.007, P = 0.016, **Figure 1G**) and global H3K27me2/H3K14Ac ratio (7.08±29.99 versus 0.22±0.26, P = 0.045, **Figure 1H**) were significantly increased in TB patients as compared with that in HS.

Gene and protein expression changes of specific histone modifying enzymes responsible for the global histone methylation/acetylation patterns

HDAC1 gene expression levels were significantly higher in TB patients than that in healthy controls (fold change 135.7±234.7 versus 7.1±13.1, P < 0.001, **Figure 2A**), while *KDM6B* (fold change 0.09±0.67 versus 5.3±15.7, P = 0.004, **Figure 2B**) gene expression levels were significantly lower in TB patients than that in HS. No significant difference in gene expression levels of *KDM1A* (fold change 4±15.4 versus 6.8±13.8, P = 0.4), *EZH2* (fold change 12.9±48 versus 33.5±169.8, P = 0.356), and *HDAC2* (fold change 29.9±106.7 versus 12.8±42.6, P

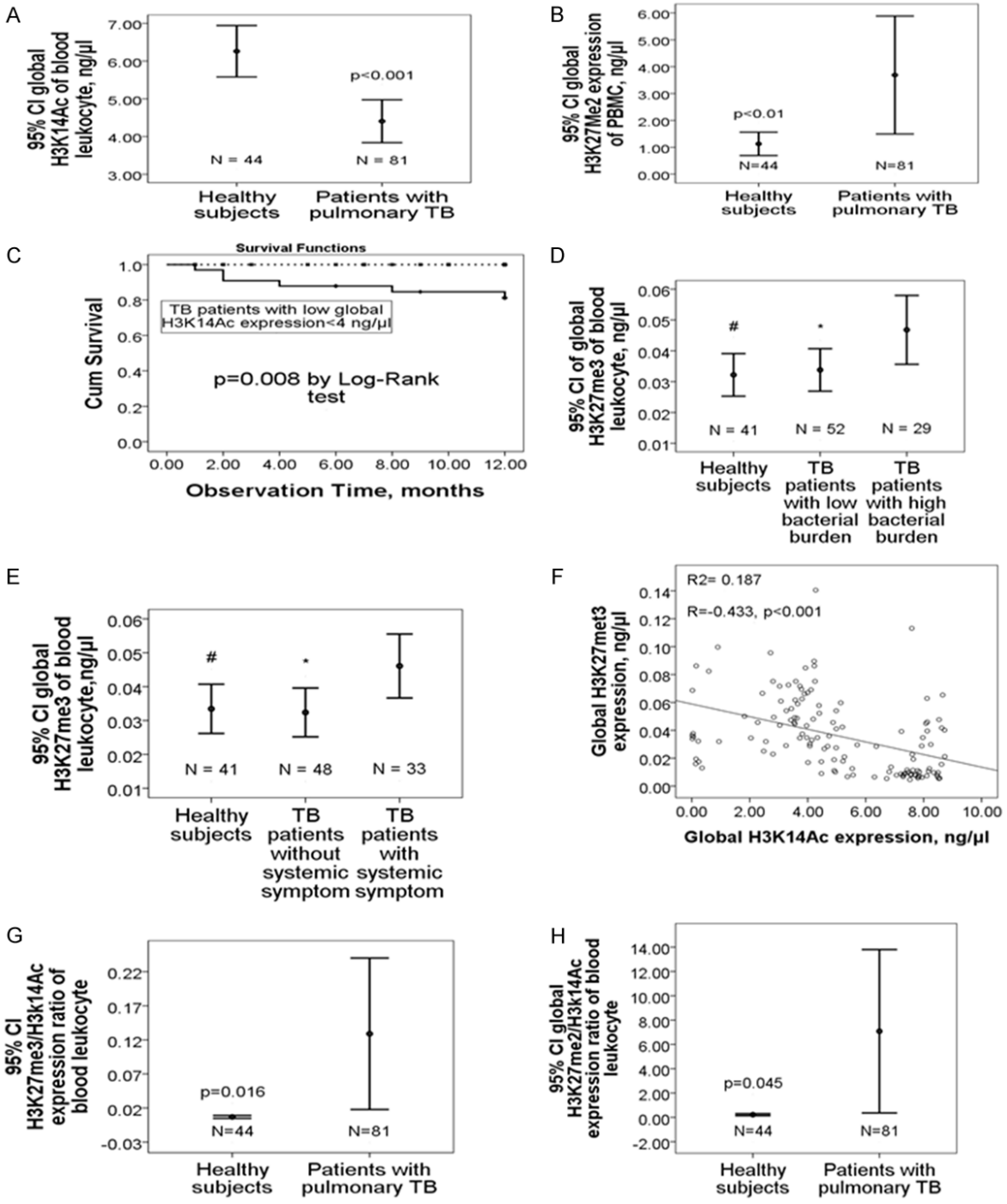

Figure 1. Global H3K14Ac, H3K27me2, and H3K27me3 expressions of blood leukocytes in patients with active pulmonary TB disease and healthy subjects (HS). The error bars show 95% confidence interval (CI) and mean. Compared with HS, (A) global H3K14Ac was significantly decreased, and (B) global H3K27me2 was increased in TB patients. (C) TB patients with a low H3K14Ac expression had lower one-year survival than those with a high value (P = 0.008, by Log-Rank test). TB patients with (D) high bacterial burden (sputum AFB 2+ to 4+) or (E) systemic symptoms (BWL or fever) had significantly increased H3K27me3 expression than those without this phenotype or HS. (F) Global H3K14Ac expression was negatively correlated with H3K27me3 expression (r = 0.433, P < 0.001). Both (G) global H3K27me3/H3K14Ac and (H) H3K27me2/H3K14Ac expression ratios were significantly increased in TB patients as compared with that in HS.

= 0.384) were found between TB patients and HS groups. HDAC1 gene expression was negatively correlated with global H3K14Ac expression (r = -0.417, P = 0.038).

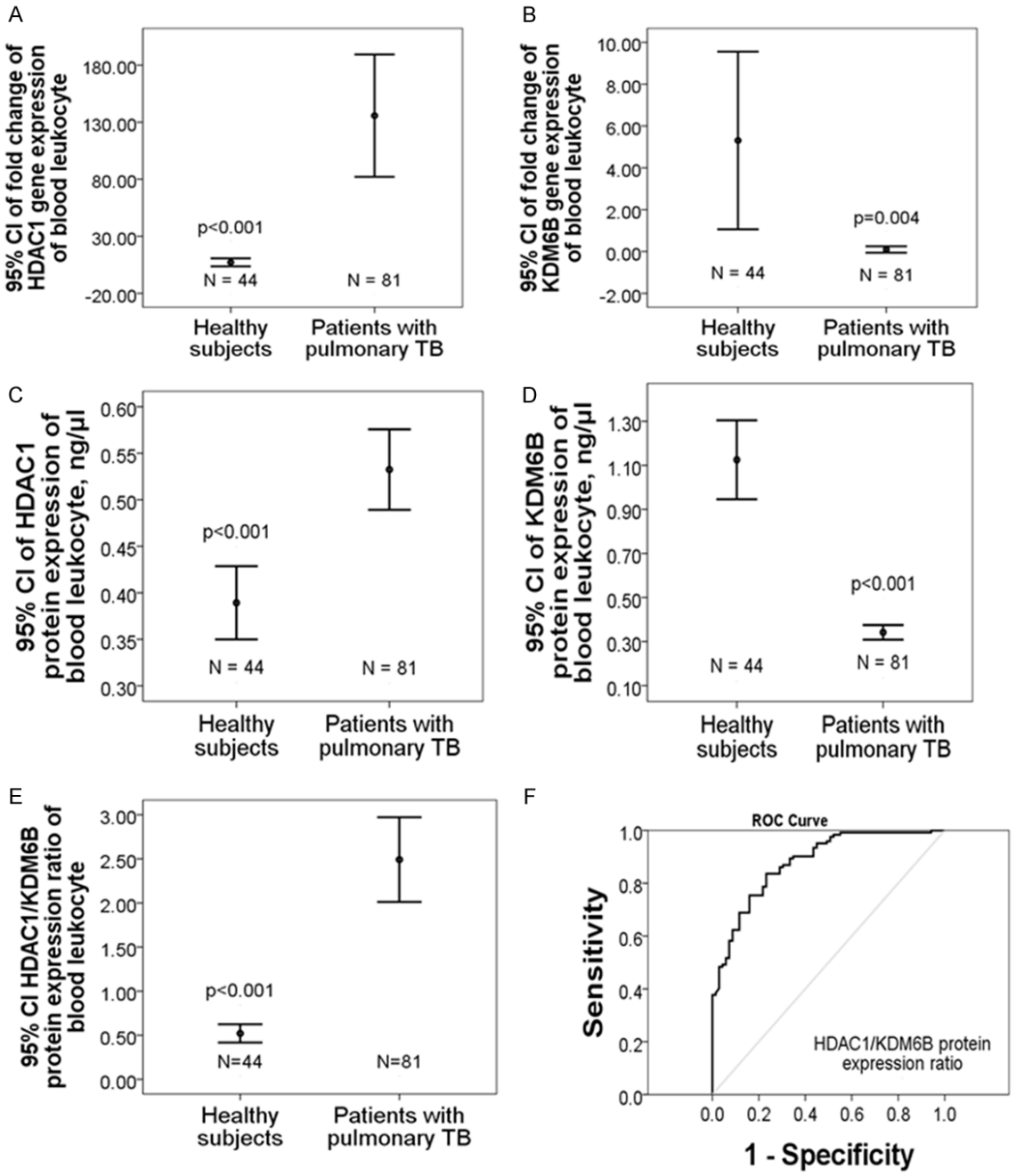

Figure 2. HDAC1 and KDM6B gene/protein expressions of blood leukocytes in patients with active pulmonary TB disease and HS. The error bars show 95% CI and mean. (A) *HDAC1* gene expression levels were significantly increased, and (B) *KDM6B* gene expression levels were decreased in TB patients as compared with that in HS. (C) HDAC1 protein expression levels were significantly increased, and (D) KDM6B protein expression levels were decreased in TB patients as compared with that in HS. (E) HDAC1/KDM6B protein expression ratio was significantly increased in TB patients as compared with that in HS. (F) The corresponding ROC curves showed that the diagnostic performance was well captured by HDAC1/KDM6B protein expression ratio (AUC = 0.879±0.025, 95% CI 0.831-0.928, P < 0.001).

HDAC1 protein expression levels were significantly higher in TB patients than that in HS (0.53±0.24 versus 0.39±0.16 ng/µl, P < 0.001, **Figure 2C**), while KDM6B protein expression levels was significantly lower in TB patients than that in HS (0.34±0.18 versus 1.13±0.75

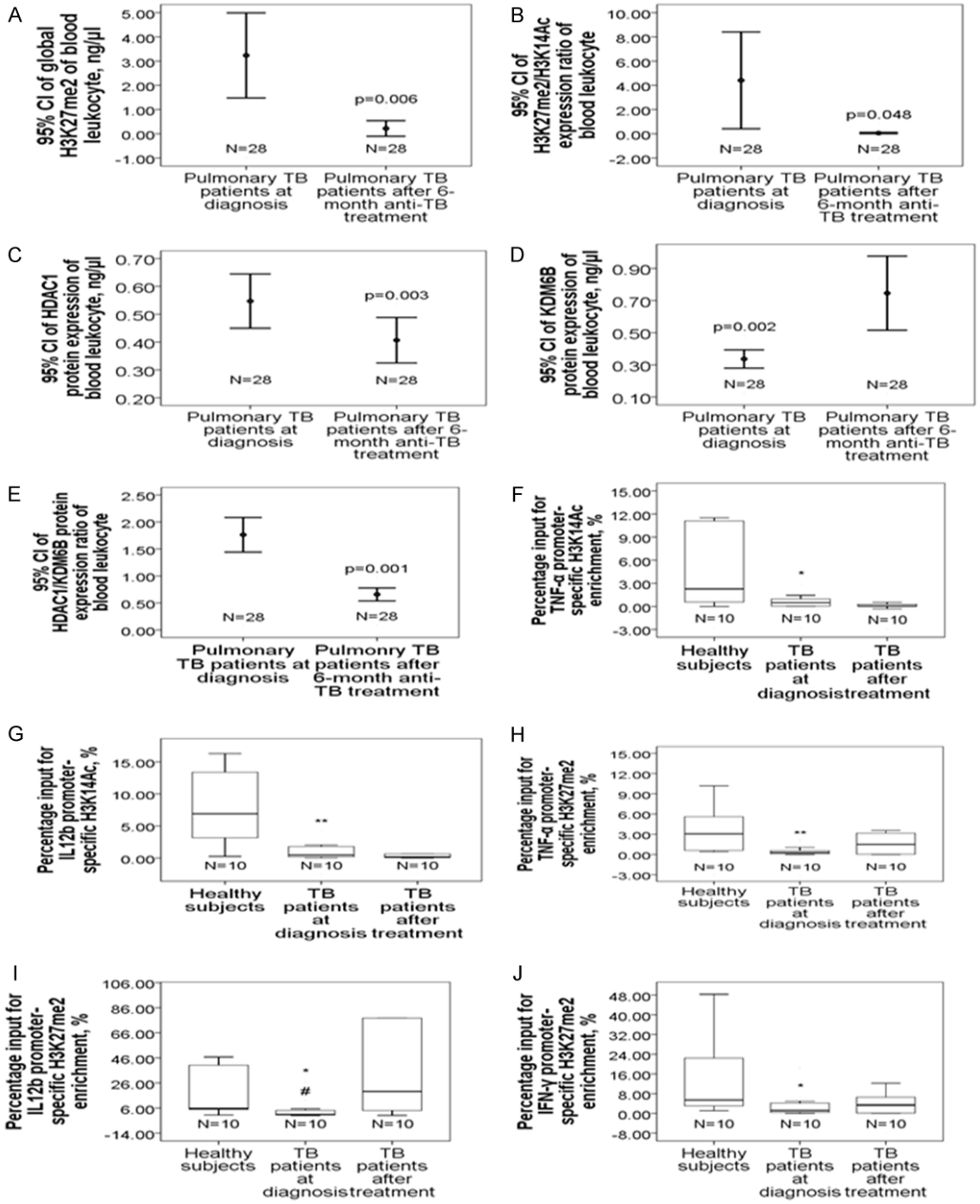

Figure 3. Changes in global H3K27me2, HDAC1 protein, KDM6B protein expressions, and gene-specific H3K14Ac/H3K27me2 enrichment in pulmonary TB patients before and after 6-month anti-TB treatment. The error bars show 95% CI and mean. Both (A) global H3K27me2 and (B) H3K27me2/H3K14Ac expression ratio showed significant reduction after therapy. (C) HDAC1 protein expression showed significant reduction, (D) KDM6B protein expression showed significant elevation, and (E) HDAC1/KDM6B protein expression ratio showed significant reduction after therapy. (F) *TNF-α* promoter-specific and (G) *IL12B* promoter-specific H3K14AC enrichment were both decreased in active TB patients, and remained depressed after anti-TB treatment. (H) *TNF-α* promoter-specific, (I) *IL12B* promoter-specific, and (J) *IFN-γ* promoter-specific H3K27me2 enrichment were all decreased in active TB patients, and the second marker was reversed to normal after anti-TB treatment. The box plots show 25th, 50th, 75th percentiles, maximal, and minimal. *P < 0.05 for comparison between TB patients and healthy subjects (HS). **P < 0.01 for comparison between TB patients and HS. #P < 0.05 for comparisons between TB patients before and after anti-TB treatment.

ng/μl, P < 0.001, **Figure 2D**). No significant difference in protein expression levels of KDM1A (0.49±1.19 versus 0.28±0.46 ng/μl, P = 0.432), EZH2 (0.61±0.3 versus 0.56±0.2 mg/ml, P = 0.293), and HDAC2 (29.5±118.2 versus 41.5±104.9 ng/μl, P = 0.585) were found between TB patients and HS groups. HDAC1 protein expression was negatively correlated with both KDM6B protein expression (r = -0.2, P = 0.004) and global H3K27me3 expression (r = -0.216, P = 0.039). KDM6B protein expression was positively correlated with global H3K14Ac expression (r = 0.693, P < 0.001). HDAC1/KDM6B protein expression ratio was significantly increased in TB patients as compared with that in HS (2.49±2.68 versus 0.52±0.43, P < 0.001, **Figure 2E**). The corresponding ROC curves showed that the diagnostic performance was well captured by HDAC1/KDM6B protein expression ratio (AUC = 0.879±0.025, 95% CI 0.831-0.928, P < 0.001, **Figure 2F**), displaying a sensitivity of 78.7% and specificity of 78.3% at a cut-off of 0.735.

Changes in global histone patterns and their corresponding enzyme expression after 6-month anti-TB treatment

In 28 TB patients whose blood samples were obtained again after 6-month anti-TB treatment, both H3K27me2 expressions (0.22±0.84 versus 1.46±4.16 ng/μl, mean difference 1.23±4.28 ng/μl, P = 0.006, **Figure 3A**) and H3K27me2/H3K14Ac ratio (2.54±6.2 versus 0.06±0.13, mean difference 2.48±1.19, P = 0.048, **Figure 3B**) were significantly reduced after therapy. No significant change in global H3K14Ac, H3K9Ac, H3K27me3, or H3K9me3 expressions was found before and after treatment. HDAC1 protein expression levels were significantly reduced after therapy (0.41±0.22 versus 0.55±0.27 ng/μl, mean difference 0.14±0.24 ng/μl, P = 0.003, **Figure 3C**), while KDM6B (0.75±0.63 versus 0.34±0.16 ng/μl, mean difference -0.41±0.65 ng/μl, P = 0.002, **Figure 3D**) protein expression levels were significantly elevated after therapy. HDAC1/KDM6B protein expression ratio was significantly reduced after therapy (2.11±2.08 versus 0.66±0.33, mean difference 1.46±2.14, P = 0.001, **Figure 3E**). No significant difference in EZH2, HDAC2, or KDM1A protein expression was found before and after treatment. There was no significant difference in gene expressions of *HDAC1, HDAC2, KDM6B, EZH2,* or *KDM1A* before and after treatment.

Decreased TNF-α/IFN-γ/IL12B promoter-specific H3K14Ac and H3K27me2 enrichment in patients with active pulmonary TB

Based on the findings that global H3K14Ac was decreased and global H3K27me2 was increased in patients with active pulmonary TB, we next investigated whether such hypoacetylation or hypermethylation occurred specifically at the promoter regions of the *TLR2, TNF-α, IFN-γ*, and *IL12B* genes. We examined this possibility by ChIP method in PBMC lysates from 10 TB patients before and after 6-month anti-TB treatment, and 10 HS, using ChIP method. The immunoprecipitated DNA pools were then assayed for the promoter sequences of the 4 selected genes (-300 to +30 bp from TSS) by PCR and real-time quantitative RT-PCR. H3K14Ac enrichment over the *TNF-α* (1.1±2.1% vs. 7.6±11.7%, P = 0.027, **Figure 3F**) and *IL12B* (1.6±2.8% vs. 7.9±6.1%, P = 0.009, **Figure 3G**) promoter regions were decreased in 10 active TB patients at diagnosis as compared with that in 10 age- and gender-matched HS, and remained depressed after 6-month anti-TB treatment. H3K27me2 enrichment over the *TNF-α* (2.1±5.4% vs. 4.6±5.4%, P = 0.005), *IL12B* (4.1±6.6% vs. 17.8±20.2%, P = 0.019), and *IFN-γ* (2.0±2.0% vs. 14.8±17.5, P = 0.027) (**Figure 3H-J**) promoter regions were all decreased in TB patients at diagnosis as compared with that in HS, and *IL12B*-specific H3K27me2 enrichment was reversed to normal after treatment (P = 0.011).

Discussion

Histone posttranslational modifications control eukaryotic gene expression and regulate many biological processes including immune cell differentiation and host immunity against pathogens [26]. Specific chromatin remodeling at specific loci, such as H3K9me3, H3K27me3/me2, and H3K9Ac, are involved in human innate and adaptive immune responses [27, 28], both of which are essential for infected individuals to eradicate MTB. Specific enzymes responsible for histone modifications, such as HDAC1, HDAC2, KDM6B, EZH2, and KDM1A play a role in antigen-specific T cell response to bacteria, parasites, or viruses [14, 15, 29-31], which is required to limit proliferation of Mtb. Our data suggest a potential role of H3K14Ac and H3K27me2/3 along with HDAC1 and KDM6B in host immune responses against Mtb.

This study is the first to find a link between global/TNF-α/IL12b-specific H3K14 hypoacetylation and active pulmonary TB infection. In line with the present findings, another intracellular bacterial pathogen, *Legionella pneumophila*, uses a Dot/Icm type IV secreted effector (RomA) to increase H3K14me3 and hence decrease H3K14 acetylation, repressing host immune defense gene expression and promoting efficient intracellular replication of the bacteria [32]. In contrast, selective enrichment of acetylated histone H3K14 at the promoter of immune genes, including TLR2, TLR4, and TLR9, is associated with Escherichia coli and Staphylococcus aureus-induced mastitis in mice [18, 33]. Additionally, HDAC3-mediated histone H3K9/K14 deacetylation is required for attenuation of interferon-α gene transcription during viral infection [34]. Furthermore, Rv3423.1, a histone acetyltransferase from virulent Mtb, has been identified recently, acetylating histone H3 at the K9/K14 positions [35]. Taken together, we speculate that Mtb may use an unknown secreted protein to decrease H3K14 acetylation and silence host immune defense genes, such as TNF-α and IL2b, therefore promoting intracellular replication of Mtb.

In parallel with the finding of global H3K14 hypoacetylation in active TB Disease in the present study, HDAC1 was up-regulated in active TB patients and reversed to normal after anti-TB treatment. HDAC1 has been shown to maintain integrity of $CD4^+$ T cell, and is required for an efficient in vivo expansion and activation of $CD8^+$ T cells in response to lymphocyte choriomeningitis virus infection [29, 36]. Furthermore, HDAC2 and HDAC3 contribute to repression of human immunodeficiency virus type 1 long terminal repeat expression, while expression of HDAC1 and 2 by macrophages is required to mount a type I interferon response to incoming γ herpesvirus [13, 37]. On the other hand, Mtb infection has been demonstrated to induce HDAC1-Mediated suppression of IL-12B gene expression through H3 hypoacetylation in macrophages in a recent in vitro study [38]. Taken together, we speculate that HDAC1 may play a divergent role in human adaptive and innate immunity against Mtb infection probably through modulating histone acetylation of immune genes.

In the present study, global H3K27me2 was increased in TB patients, and H3K27me3 was increased in TB patients with high bacterial burden or systemic symptoms, while H3K27me2/me3-specific demethylase, KDM6B, was down-regulated in TB patients. Both H3K27me2 and KDM6B protein expressions were reversed to normal after anti-TB treatment. Consistent with our findings, KDM6B (JMJD3) has been shown to contribute to the control of gene expression in lipopolysaccharide-activated macrophages in a H3K27 demethylation-independent manner [39]. Furthermore, the genome of the *herpes simplex virus 1* (*HSV-1*) during latency is associated with H3K27me3 marks, and KDM6B contribute to the ability of HSV-1 to become reactivated in sensory neurons [40]. KDM6B is also imperative for M2 macrophage polarization in response to parasitic helminth infections [14].

Recently, Rv1988, a secreted mycobacterial protein, has been demonstrated to dimethylate histone H3 at H3Arginine(R) 42 and represses the genes involved in the first line of defense against mycobacteria [41]. Taken together, we speculate that H3K27me2 and KDM6B may promote and inhibit the reactivation of pulmonary TB, respectively, whereas H3K27me3 may mark the infection of Mtb, especially severe clinical phenotypes. The paradoxically decreased enrichment of H3K27me2 over the *IL12B* promoter region in active TB patients and its reversion after treatment may indicate a protective immune response to overcome H3K14 hypoacetylation induced by Mtb. A recent study reported that TNF-α decreased H3K27 acetylation and increased H3K27 dimethylation at the *IL12B* promoter region, which might contribute to *IL12B* trans-suppression by lincRNA-Cox2, while another study demonstrated that histone acetylation at promoters and enhancers at the *TNF-α* and *IL12B* loci did not activate transcription but greatly increased and prolonged recruitment of TLR-induced transcription factors and RNA polymerase II to gene promoters and enhancers [42, 43]. The exact epigenetic mechanisms by which Mtb induce protective and pathogenic immune responses in human beings require further investigation.

The possible limitations of this study should be acknowledged. First, the causal relationship between histone medication/enzyme changes and active TB infection is not straightforward in this association study, although the reversion of KDM6B and HDAC1 after treatment indicates that Mtb activation leads to dynamic

change of these two enzymes. Second, the causal relationship between H3K14Ac/H3K27me3 and their corresponding enzyme HDAC1/KDM6B expressions is not straightforward. Based on literature review, the up-regulation of HDAC1 and down-regulation of KDM6B may be responsible for H3K14 hypoacetylation and H3K27 hypermethylation in active or severe phenotypes of pulmonary TB, respectively. Further in vitro investigation is required to clarify these cause and effect relationships. Third, these potential biomarkers were not examined in latent TB subjects. A large longitudinal cohort, including uninfected healthy subjects, latent TB, active TB, and TB patients after treatment, is required to clarify their roles in the switch from Mtb infection to reactivation statuses. Nonetheless, the results indicate that histone H3K27me/H3K14Ac marks may be important targets for inhibition of Mtb reactivation, offering new insights into improving the efficacy of immunotherapy or vaccination for pulmonary TB. Finally, other immunological genes with H3K14 hypoacetylation or H3K27 hypermethylation were not examined. A whole-genome survey of H3K14Ac and H3K27me2 enrichment is ongoing to identify novel immunological genes, with which M.tb may interact through histone modifications.

In summary, global H3K14 hypoacetylation, global H3K27 hyperdimethylation, *TNF-α/IL12B* promoter-specific H3K14 hypoacetylation, and *TNF-α/IL12b/IFN-γ* promoter-specific H3K27 hypodimethylation were found along with HDAC1 up-regulation and KDM6B down-regulation in patients with active pulmonary TB disease. Several histone modification markers, including global H3K27me2, HDAC1, KDM6B, and *IL12B* promoter-specific H3K27me2, were reversed to normal after 6-month anti-TB treatment, and some were correlated with severe phenotypes. Histone methylation and acetylation of immune genes, such as TNF-α, IFN-γ and IL12-B, may play a role in human immune responses against Mtb infection, but further investigation is required to clarify these gene-specific histone Ac/me statuses in active TB, latent TB, and healthy non-infected subjects.

We conclude that global H3K14 hypoacetylation and H3K27 hypermethylation in active pulmonary TB patients indicate a novel epigenetic modulation for Mtb to subvert the human immune system. Increased HDAC1/KDM6B ratio and decreased global H3K14Ac may serve as potential biomarkers for disease diagnosis and poor prognosis of active pulmonary TB disease, respectively. Additionally, decreased TNF-α/IL12B promoter-specific H3K14Ac enrichment in active TB patients substantiates the recent predictions that HDAC inhibitors can be potential therapeutic agents to control Mtb infection.

Acknowledgements

This work was supported by grants from the Ministry of Science and Technology, Taiwan (NMRPG8D6132 to M.C. Lin, and NMRPG8B0151/101-2314-B-182A-092 to Y.C. Chen) and from Chang Gung Memorial Hospital (CMRPG8C1182 to M.C. Lin, and CMRPG8D1571/CMRPG8E1091 to Y.C. Chen), Taiwan. The authors acknowledge the technical support provided by the Genomic and Proteomic Core Laboratory, and the Internal Medicine Core Facility of the Kaohsiung Chang Gung Memorial Hospital.

Disclosure of conflict of interest

None.

Address correspondence to: Dr. Meng-Chih Lin, Division of Pulmonary and Critical Care Medicine, Kaohsiung Chang Gung Memorial Hospital and Chang Gung University College of Medicine, 123, Ta-Pei Rd, Niao-Sung District, Kaohsiung City, Taiwan. Tel: +886-7-7317123 Ext 8199; Fax: +886-7-7322402; E-mail: linmengchih@hotmail.com; Chang-Chun Hsiao, Graduate Institute of Clinical Medical Sciences, College of Medicine, Chang Gung University, Center for Shockwave Medicine and Tissue Engineering, Kaohsiung Chang Gung Memorial Hospital, Taiwan. E-mail: cchsiao@mail.cgu.edu.tw

References

[1] Dheda K, Barry CE 3rd and Maartens G. Tuberculosis. Lancet 2016; 387: 1211-26.
[2] Sia JK, Georgieva M and Rengarajan J. Innate immune defenses in Human tuberculosis: an overview of the interactions between mycobacterium tuberculosis and innate immune cells. J Immunol Res 2015; 2015: 747543.
[3] Orme IM, Robinson RT and Cooper AM. The balance between protective and pathogenic immune responses in the TB-infected lung. Nat Immunol 2015; 16: 57-63.

[4] Zhao M, Wang Z, Yung S and Lu Q. Epigenetic dynamics in immunity and autoimmunity. Int J Biochem Cell Biol 2015; 67: 65-74.
[5] Chen YC, Hsiao CC, Chen CJ, Chao TY, Leung SY, Liu SF, Wang CC, Wang TY, Chang JC, Wu CC, Lin AS, Wang YH and Lin MC. Aberrant Toll-like receptor 2 promoter methylation in blood cells from patients with pulmonary tuberculosis. J Infect 2014; 69: 546-557.
[6] Chen YC, Hsiao CC, Chen CJ, Chin CH, Liu SF, Wu CC, Eng HL, Chao TY, Tsen CC, Wang YH and Lin MC. Toll-like receptor 2 gene polymorphisms, pulmonary tuberculosis, and natural killer cell counts. BMC Med Genet 2010; 11: 17.
[7] Karmodiya K, Krebs AR, Oulad-Abdelghani M, Kimura H and Tora L. H3K9 and H3K14 acetylation co-occur at many gene regulatory elements, while H3K14ac marks a subset of inactive inducible promoters in mouse embryonic stem cells. BMC Genomics 2012; 13: 424.
[8] Ezponda T and Licht JD. Molecular pathways: deregulation of histone h3 lysine 27 methylation in cancer-different paths, same destination. Clin Cancer Res 2014; 20: 5001-5008.
[9] Yasmin R, Siraj S, Hassan A, Khan AR, Abbasi R and Ahmad N. Epigenetic regulation of inflammatory cytokines and associated genes in human malignancies. Mediators Inflamm 2015; 2015: 201703.
[10] Volkel P, Dupret B, Le Bourhis X and Angrand PO. Diverse involvement of EZH2 in cancer epigenetics. Am J Transl Res 2015; 7: 175-193.
[11] Burchfield JS, Li Q, Wang HY and Wang RF. JMJD3 as an epigenetic regulator in development and disease. Int J Biochem Cell Biol 2015; 67: 148-57.
[12] Laurent B, Ruitu L, Murn J, Hempel K, Ferrao R, Xiang Y, Liu S, Garcia BA, Wu H, Wu F, Steen H and Shi Y. A specific LSD1/KDM1A isoform regulates neuronal differentiation through H3K9 demethylation. Mol Cell 2015; 57: 957-970.
[13] Keedy KS, Archin NM, Gates AT, Espeseth A, Hazuda DJ and Margolis DM. A limited group of class I histone deacetylases acts to repress human immunodeficiency virus type 1 expression. J Virol 2009; 83: 4749-4756.
[14] Satoh T, Takeuchi O, Vandenbon A, Yasuda K, Tanaka Y, Kumagai Y, Miyake T, Matsushita K, Okazaki T, Saitoh T, Honma K, Matsuyama T, Yui K, Tsujimura T, Standley DM, Nakanishi K, Nakai K and Akira S. The Jmjd3-Irf4 axis regulates M2 macrophage polarization and host responses against helminth infection. Nat Immunol 2010; 11: 936-944.
[15] Anderton JA, Bose S, Vockerodt M, Vrzalikova K, Wei W, Kuo M, Helin K, Christensen J, Rowe M, Murray PG and Woodman CB. The H3-K27me3 demethylase, KDM6B, is induced by Epstein-Barr virus and over-expressed in Hodgkin's Lymphoma. Oncogene 2011; 30: 2037-2043.
[16] Pero R, Peluso S, Angrisano T, Tuccillo C, Sacchetti S, Keller S, Tomaiuolo R, Bruni CB, Lembo F and Chiariotti L. Chromatin and DNA methylation dynamics of Helicobacter pylori-induced COX-2 activation. Int J Med Microbiol 2011; 301: 140-149.
[17] Angrisano T, Lembo F, Peluso S, Keller S, Chiariotti L and Pero R. Helicobacter pylori regulates iNOS promoter by histone modifications in human gastric epithelial cells. Med Microbiol Immunol 2012; 201: 249-257.
[18] Modak R, Das Mitra S, Krishnamoorthy P, Bhat A, Banerjee A, Gowsica BR, Bhuvana M, Dhanikachalam V, Natesan K, Shome R, Shome BR and Kundu TK. Histone H3K14 and H4K8 hyperacetylation is associated with Escherichia coli-induced mastitis in mice. Epigenetics 2012; 7: 492-501.
[19] Barton KM, Archin NM, Keedy KS, Espeseth AS, Zhang YL, Gale J, Wagner FF, Holson EB and Margolis DM. Selective HDAC inhibition for the disruption of latent HIV-1 infection. PLoS One 2014; 9: e102684.
[20] Jenke AC, Hensel KO, Klein A, Willuhn L, Prax S, Weil PP, Winkler T, Deba T, Orth V, Baiker A, Wirth S and Postberg J. Restitution of gene expression and histone acetylation signatures altered by hepatitis B virus through antiviral microRNA-like molecules in nontransformed murine hepatocytes. Clin Epigenetics 2014; 6: 26.
[21] Mounce BC, Mboko WP, Kanack AJ and Tarakanova VL. Primary macrophages rely on histone deacetylase 1 and 2 expression to induce type I interferon in response to gammaherpesvirus infection. J Virol 2014; 88: 2268-2278.
[22] Guise AJ, Budayeva HG, Diner BA and Cristea IM. Histone deacetylases in herpesvirus replication and virus-stimulated host defense. Viruses 2013; 5: 1607-1632.
[23] Lamoth F, Juvvadi PR and Steinbach WJ. Histone deacetylase inhibition as an alternative strategy against invasive aspergillosis. Front Microbiol 2015; 6: 96.
[24] Bhatnagar S, Gazin C, Chamberlain L, Ou J, Zhu X, Tushir JS, Virbasius CM, Lin L, Zhu LJ, Wajapeyee N and Green MR. TRIM37 is a new histone H2A ubiquitin ligase and breast cancer oncoprotein. Nature 2014; 516: 116-120.
[25] Haring M, Offermann S, Danker T, Horst I, Peterhansel C and Stam M. Chromatin immunoprecipitation: optimization, quantitative analysis and data normalization. Plant Methods 2007; 3: 11.

[26] Nicholas D, Tang H, Zhang Q, Rudra J, Xu F, Langridge W and Zhang K. Quantitative proteomics reveals a role for epigenetic reprogramming during human monocyte differentiation. Mol Cell Proteomics 2015; 14: 15-29.
[27] Huang Y, Min S, Lui Y, Sun J, Su X, Liu Y, Zhang Y, Han D, Che Y, Zhao C, Ma B and Yang R. Global mapping of H3K4me3 and H3K27me3 reveals chromatin state-based regulation of human monocyte-derived dendritic cells in different environments. Genes Immun 2012; 13: 311-320.
[28] Decker T, Pasca di Magliano M, McManus S, Sun Q, Bonifer C, Tagoh H and Busslinger M. Stepwise activation of enhancer and promoter regions of the B cell commitment gene Pax5 in early lymphopoiesis. Immunity 2009; 30: 508-520.
[29] Tschismarov R, Firner S, Gil-Cruz C, Goschl L, Boucheron N, Steiner G, Matthias P, Seiser C, Ludewig B and Ellmeier W. HDAC1 controls CD8+ T cell homeostasis and antiviral response. PLoS One 2014; 9: e110576.
[30] Macfarlan TS, Gifford WD, Agarwal S, Driscoll S, Lettieri K, Wang J, Andrews SE, Franco L, Rosenfeld MG, Ren B and Pfaff SL. Endogenous retroviruses and neighboring genes are coordinately repressed by LSD1/KDM1A. Genes Dev 2011; 25: 594-607.
[31] Sourvinos G, Morou A, Sanidas I, Codruta I, Ezell SA, Doxaki C, Kampranis SC, Kottakis F and Tsichlis PN. The downregulation of GFI1 by the EZH2-NDY1/KDM2B-JARID2 axis and by human cytomegalovirus (HCMV) associated factors allows the activation of the HCMV major IE promoter and the transition to productive infection. PLoS Pathog 2014; 10: e1004136.
[32] Rolando M, Sanulli S, Rusniok C, Gomez-Valero L, Bertholet C, Sahr T, Margueron R and Buchrieser C. Legionella pneumophila effector RomA uniquely modifies host chromatin to repress gene expression and promote intracellular bacterial replication. Cell Host Microbe 2013; 13: 395-405.
[33] Modak R, Das Mitra S, Vasudevan M, Krishnamoorthy P, Kumar M, Bhat AV, Bhuvana M, Ghosh SK, Shome BR and Kundu TK. Epigenetic response in mice mastitis: role of histone H3 acetylation and microRNA(s) in the regulation of host inflammatory gene expression during staphylococcus aureus infection. Clin Epigenetics 2014; 6: 12.
[34] Genin P, Lin R, Hiscott J and Civas A. Recruitment of histone deacetylase 3 to the interferon-A gene promoters attenuates interferon expression. PLoS One 2012; 7: e38336.
[35] Jose L, Ramachandran R, Bhagavat R, Gomez RL, Chandran A, Raghunandanan S, Omkumar RV, Chandra N, Mundayoor S and Kumar RA. Hypothetical protein Rv3423.1 of mycobacterium tuberculosis is a histone acetyltransferase. FEBS J 2016; 283: 265-281.
[36] Boucheron N, Tschismarov R, Goschl L, Moser MA, Lagger S, Sakaguchi S, Winter M, Lenz F, Vitko D, Breitwieser FP, Muller L, Hassan H, Bennett KL, Colinge J, Schreiner W, Egawa T, Taniuchi I, Matthias P, Seiser C and Ellmeier W. CD4(+) T cell lineage integrity is controlled by the histone deacetylases HDAC1 and HDAC2. Nat Immunol 2014; 15: 439-448.
[37] Mounce BC, Mboko WP, Bigley TM, Terhune SS and Tarakanova VL. A conserved gammaherpesvirus protein kinase targets histone deacetylases 1 and 2 to facilitate viral replication in primary macrophages. J Virol 2013; 87: 7314-7325.
[38] Chandran A, Antony C, Jose L, Mundayoor S, Natarajan K and Kumar RA. Mycobacterium tuberculosis infection induces HDAC1-mediated suppression of IL-12B gene expression in macrophages. Front Cell Infect Microbiol 2015; 5: 90.
[39] De Santa F, Narang V, Yap ZH, Tusi BK, Burgold T, Austenaa L, Bucci G, Caganova M, Notarbartolo S, Casola S, Testa G, Sung WK, Wei CL and Natoli G. Jmjd3 contributes to the control of gene expression in LPS-activated macrophages. EMBO J 2009; 28: 3341-3352.
[40] Messer HG, Jacobs D, Dhummakupt A and Bloom DC. Inhibition of H3K27me3-specific histone demethylases JMJD3 and UTX blocks reactivation of herpes simplex virus 1 in trigeminal ganglion neurons. J Virol 2015; 89: 3417-3420.
[41] Yaseen I, Kaur P, Nandicoori VK and Khosla S. Mycobacteria modulate host epigenetic machinery by Rv1988 methylation of a non-tail arginine of histone H3. Nat Commun 2015; 6: 8922.
[42] Tong Q, Gong AY, Zhang XT, Lin C, Ma S, Chen J, Hu G and Chen XM. LincRNA-Cox2 modulates TNF-alpha-induced transcription of Il12b gene in intestinal epithelial cells through regulation of Mi-2/NuRD-mediated epigenetic histone modifications. FASEB J 2016; 30: 1187-1197.
[43] Qiao Y, Giannopoulou EG, Chan CH, Park SH, Gong S, Chen J, Hu X, Elemento O and Ivashkiv LB. Synergistic activation of inflammatory cytokine genes by interferon-gamma-induced chromatin remodeling and toll-like receptor signaling. Immunity 2013; 39: 454-469.